Sustainable Solutions for Heavy Metal Contamination: Characterization and Regeneration of Water Hyacinth Biosorbent in Wastewater Treatment

Rabiranjan Murmu[1], Santhi M. George[2]*, Yuvarani P.[3], Priyanka Bhatnagar[4], Amudha K.[5] and Karuna M. S.[6]

[1]Department of Chemical Engineering, Indira Gandhi Institute of Technology, Sarang, Odisha 759146, India

[2]*Department of Science and Humanities, RMK Engineering College, Tamil Nadu 601206, India

[3]Department of Electronics and Communication Engineering, M.Kumarasamy College of Engineering, Karur, Tamil Nadu 639113, India

[4]School of Basic & Applied Sciences, IILM University, Greater Noida, Uttar Pradesh 201306, India

[5]Department of Science and Humanities-Physics, R.M.D. Engineering College (An Autonomous Institution), Kavaraipettai, Tamil Nadu 601206, India
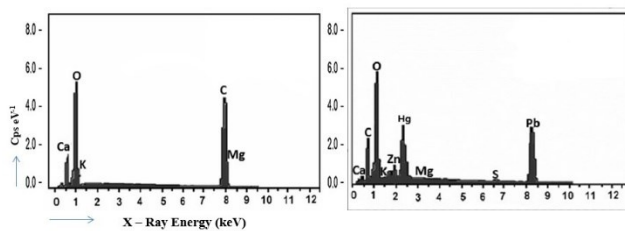
[6]Department of Chemical Engineering, M.J.P. Rohilkhand University, Bareilly, Uttar Pradesh 243006, India

Graphical abstract

Abstract

The water hyacinth biosorbent has undergone thorough characterization and assessment for its capacity to remove heavy metals, specifically Pb(II) and Hg(II) from aqueous solutions. Notably, the biosorbent demonstrated an impressive maximum adsorption capacity for Pb and Hg, reaching values of 158.7 mg/g and 123.5 mg/g, respectively. Indeed, these adsorption capacities align with or even surpass those documented in the existing literature for various biosorbents derived from similar agro-industrial waste materials. Several methods were used to characterize the water hyacinth biosorbent's structure and morphology, including pH-Zero Point Change, scanning electron microscopy/energy-dispersive X-ray spectroscopy (SEM/EDS), and infrared spectrometry with Fourier transform (FT-IR). The water hyacinth biosorbent was found to have broken exteriors with mixed particles that involved useful adsorption clusters such as OH, C=O, and C-O-C. The most effective adsorption of Pb(II) and Hg(II) takes place at a pH of 5.0, using a hyacinth dose of 2 g/L. The chemisorption process is the primary cause of the fast growth rate of the adsorption process, which is governed by pseudo-second-order kinetics. Using a 0.1M HNO_3 eluent, both biosorbents were effectively regenerated, enabling effective reuse for up to five cycles. The thermodynamic studies confirm the endothermic nature of the adsorption process.

Keywords: Water Hyacinth, Biosorption, Batch studies, Kinetic and Equilibrium studies, Thermodynamic studies.

1. Introduction

Water pollution refers to the contamination of water bodies, such as rivers, lakes, oceans, groundwater, and other aquatic systems, resulting in adverse effects on the environment, human health, and aquatic ecosystems. This pollution can be caused by various pollutants entering water sources through natural processes or human activities (Kaparapu *et al.* 2018). One of the main issues that is currently gaining international attention is the anthropogenic pollution of the water environment. Aquatic ecosystems are indeed vulnerable to pollution from various sources, including industrial activities, agriculture, urban runoff, and improper disposal of waste (Priya *et al.* 2022). This pollution can introduce a range of contaminants, including heavy metals, pesticides, nutrients, and organic pollutants, into water bodies, leading to adverse effects on aquatic life and ecosystems. Aquatic ecosystems are seriously threatened by inorganic contaminants, which can come from a variety of sources including mining operations, metal structure corrosion, and industrial processes like electroplating and battery production. Mining activities, for instance, contribute to water contamination through the leaching of heavy metals like lead, mercury, and cadmium (Hong *et al.* 2020).

The rusting of metal structures releases iron oxide into the water, impacting water quality. Industries engaged in electroplating and battery manufacture discharge heavy metals such as chromium, cadmium, and nickel, which can be harmful to aquatic life and accumulate in the food chain. The toxicity, durability, and capacity for bioaccumulation of

heavy metals in the food chain of living organisms make them particularly harmful. Lead (Pb) and Mercury (Hg) can cause serious health problems when consumed, especially in the brain system and reproductive systems (Manjuladevi *et al.* 2018). These metal ions have both natural and anthropogenic sources. While they have certain industrial applications, the release of lead and mercury into the environment poses significant risks to human health and the ecosystem due to their toxicity (Haro *et al.* 2021). Investigating heavy metal adsorption mechanisms on bio surfaces or biosorbent substances, as well as the successful removal of Pb and Hg from wastewater, is therefore highly relevant at this time. Because these materials are readily available and the cost of treating contaminated water is inexpensive, using them is appealing (Ma *et al.* 2022).

Water hyacinth (Eichhornia crassipes) is a free-floating aquatic plant known for its rapid growth and ability to spread across water bodies. While it is native to the Amazon basin, water hyacinth has become a highly invasive species in many regions around the world. It has been utilized in various parts of the world for wastewater treatment due to its ability to absorb nutrients, including nitrogen and phosphorus, and its potential to improve water quality. Despite its potential benefits, the use of water hyacinth in wastewater treatment requires careful consideration of ecological impacts and local conditions (Eleryan *et al.* 2022). Uncontrolled growth of water hyacinth can lead to issues such as clogging of waterways and interference with native plant and animal species. Therefore, its use should be integrated into well-managed and monitored systems to ensure effective wastewater treatment while minimizing negative consequences.

The current experimental investigation aims to assess the water hyacinth biosorbent's adsorption behaviour for the removal of Pb(II) and Hg(II) metal ions from the synthetically generated solution. The optimal values for several adsorption parameters were found using the batch method of adsorption, and kinetic and equilibrium experiments were used to assess the effectiveness of the adsorption process. The wasted adsorbent was reused up to five times during the elution investigations, which were carried out using five distinct types of acids in varying cycles.

2. Methods

2.1. Preparation of biosorbents

Water Hyacinth biochar agro-industrial wastes were gathered from the Junin, Peruvian provinces of Chanchamayo and Satipo. Before being dried at 70°C for 48 hours, the samples were first cleaned with water and then rinsed with distilled water. Subsequently, a 70-mesh sieve was used to grind and strain the dried absorbents. Every chemical and reagent utilized in this investigation was of analytical grade. A mixture of 50 mL of aqueous solutions and 0.05 mg of biosorbent was generated at various beginning pHs (pH_0), ranging from 1 to 8. The 1M HCl solution was used to prepare the acid dilutions and 1M NaOH was used to prepare the basic dilutions. We calculated the final pHs (pH_f) during 24 hours of

equilibrium. Biosorbent surface functional groups were characterized using a Fourier transform infrared spectrophotometer (FTIR, SHIMADZU-8700). Between 4000 and 400 cm-1 was the wavelength selected. Scanning electron microscopy (SEM) in conjunction with energy dispersive X-ray spectroscopy (EDX) (Hitachi SU8230 model) was used to analyze the morphology and elemental composition of the surface of Water Hyacinth biosorbents.

2.2. Adsorption experiments

The study investigated the influence of various experimental parameters, including pH, hyacinth biochar dose, reaction time, Pb and Hg concentration, and kinetic and isothermal models. 25 mL of $PbSO_4$ and $Hg(NO_3)_2$ solution was mixed with 0.025–0.2 g of each biosorbent, resulting in a range of [Pb and Hg] values between 26.9 and 196.4 mg/L. The pH of these solutions was brought to a range of 2.0–5.0 with the addition of 0.1M HNO_3 or 0.1M NaOH. For a 0–120 minutes, the suspension was agitated at 200 rpm. It was maintained at room temperature. By utilizing the Hitachi SU8230 (AAS) instrument, the amount of lead and mercury that was adsorbable onto the biosorbents was measured. The following equations (1 & 2) were used to compute the adsorption capacity q_e (in mg/g) and removal efficiency (%R) correspondingly:

$$q_e = \frac{C_o - C_e}{m} V \tag{1}$$

$$\%R = \frac{C_o - C_e}{C_o} x100 \tag{2}$$

where m (in g) is the mass of the biosorbent, V (in L) is the volume of solution, and Ce (in mg/L) is the equilibrium final Pb and Hg concentration. The average values obtained from the three repetitions of the adsorption tests were reported. The models of pseudo-first order, pseudo-second order Largergren, and intraparticle-diffusion were used to assess the kinetic data. The adsorption isotherms' experimental data were connected with the Freundlich Eq. (4), and Langmuir Eq. (3), models.

$$\frac{C_e}{q_e} = \frac{1}{b q_{max}} + \frac{C_e}{q_{max}} \tag{3}$$

The Langmuir constants b and q_{max} correspond to the maximal biosorption capacity and the affinity between sorbent-sorbate, respectively.

$$\ln q_e = \ln k_f + \frac{1}{n} \ln C_e \tag{4}$$

where equilibrium and the affinity between sorbent and sorbet are linked to k_f and n.

2.3. Desorption experiments

Five different 0.1M eluent acid types (HCl, HNO_3, H_2SO_4, CH_3COOH, and NaOH) were used in the desorption procedure. For desorption studies, 50 mL of the above-mentioned eluents were mixed with 100 mg of water hyacinth biosorbent loaded with pb and Hg metal ions (C_0 = 75.8 mg/L). Around 50 mL of Pb and Hg-loaded water hyacinth biosorbent was used for this study and then it was filtered & dried. The mixture was then agitated at 200 rpm for two hours. The biosorbents were then dried, cleaned

with distilled water, and utilized once more. Up to six times did the adsorption/desorption process occur. Utilizing atomic absorption spectroscopy, the concentration of adsorbed and desorbed Pb and Hg was determined. The following equation 5, is used to calculate the desorption efficacy (%Des) of the water hyacinth biosorbent under study:

$$\%D = \frac{Metal\ ions\ desorbed}{Metal\ ions\ sorbed} x100 \qquad (5)$$

3. Results and Discussion

3.1. Properties of biosorbent and effect of pH

When ΔpH (pH_0 - pH_f) is plotted against the initial pH_0 values, the zero charge point pH values (pH_{ZPC}) can be found (see Figure 1). Equating to pH_{ZPC} = 4.8, the curve associated with the Water Hyacinth biochar cross the pH_0 axis. This suggests that the Water Hyacinth biochar surfaces have a positive charge at a pH value of 4.9. The biosorbent surface has a negative charge when the pH is higher than pH_{ZPC} (Saeed *et al.* 2020).
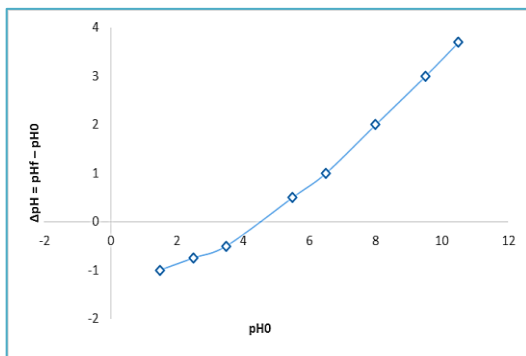

Figure 1. pH_{ZPC} determination for water hyacinth biosorbent

At higher pH values, Pb and Hg are electrostatically attracted to one another. It is important to emphasize how pH impacts the ability of Pb and Hg uptake since pH influences the adsorbent's external features, such as charged surfaces, ion contents, and the functional group's dispersion levels on the biochar's sites (Su *et al.* 2021).
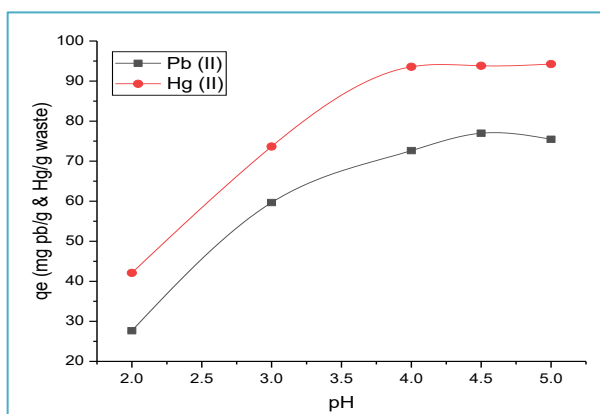


Figure 2. pH influence for Pb and Hg removal capacity
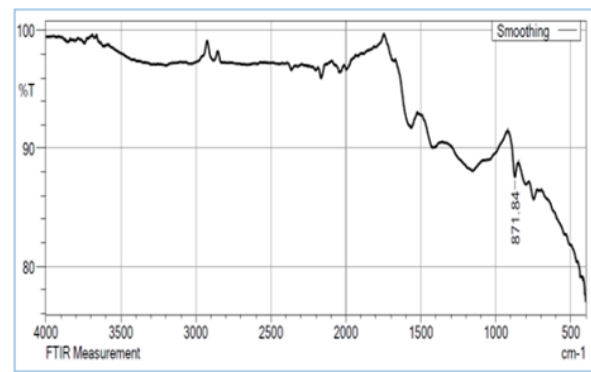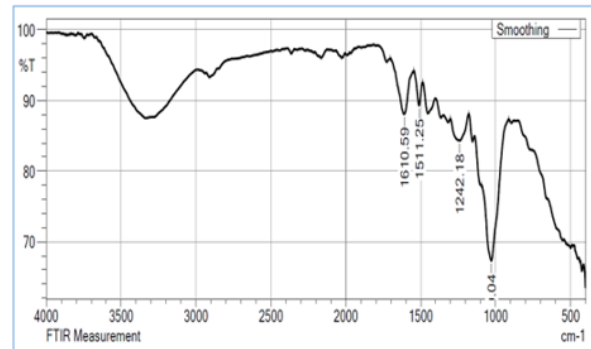
**Figure 3.** FTIR spectra of before (a) and after (b) of metal ion adsorption

The effect of Pb and Hg sorption capacity q_e's pH on Water Hyacinth biochar is depicted in Figure 2. Therefore, at acidic pHs, we recognize that the biosorbent's adsorption ability, qe, increases and reaches a maximum around pH = 5. This tendency is connected to the battle for biosorbent active sites between H_3O^+ and Pb and Hg ions (Langeroodi *et al.* 2018). As a result, when pH is less than pH_{ZPC}, there is a significant concentration of H_3O^+ ions, which can occupy the majority of the biosorbent active sites (Khan *et al.* 2022). In this case, the adsorbent's ability to absorb Pb and Hg ions is diminished since it repels them. The pH > pH_{ZPC} scenario is the opposite, as this enhances the Pb and Hg adsorption capacity q_e of the biosorbent due to its negative surface (Ma *et al.* 2022). In our instance, we discovered that Pb and Hg were being removed at an increasing rate up to pH 5, yet even at these tiny values, Pb and Hg were precipitating quickly. According to the Pb and Hg-Pourbaix diagram, Pb and Hg precipitation to Pb and Hg (OH)$_2$ is the cause of the suppression of Pb and Hg bio adsorption reported in the literature above pH 5–6 (Ambaye *et al.* 2021). Functional groups on the surface of Water Hyacinth charcoal biosorbents were identified, and FTIR spectrum analysis was used to investigate relationships among these groups and Pb and Hg ions. The characteristic FTIR spectrum of water hyacinth charcoal is shown in Figure 3, with similar peak absorption or bands of wavelengths before and following Pb and Hg adsorption. The band locations for the biosorbent without pollutants show at 3276.6 cm^{-1}, which are indicative of normal -OH bond stretching vibrations in materials like lignin and cellulose (Benjelloun *et al.* 2021). These values correspond to the balanced extending of C-H bonds that is common in lignocellulosic samples, which is 2910.2 and 1236.1 cm^{-1};

the irregular extending of the dual bond of C = O carbonyl groups is responsible for 1627.9 cm^{-1}; and assigned to the stretching C-OH (Venkatraman *et al.* 2021). Following contact with the Pb and Hg solution, some adsorption peaks' positions and intensities change, as shown in the FTIR spectra same as discussed in Wang *et al.* (2022). . Therefore, for both metal ions, the locations of the bands 1/ and 3/ are significantly shifted at Δ_1 = 15.2 (13.01) and Δ_3 = - 25.2 (12.1) cm^{-1} to the values of the clean sample. The band 5/ is significantly displaced at Δ_5 = (6.1) cm^{-1} for Water Hyacinth biochar as well. These findings suggest that Pb and Hg biosorption would involve the O-H, C-O, and C-O-C groups.

Before and after the Pb and Hg sorption operations, typical EDS spectra of Water Hyacinth biochar are displayed in Figure 4. C, O, Mg, K, and Ca are among the common elements present in both clean biosorbents. Along with Water Hyacinth biochar to Zn, Pb, Hg, and S, it also covers Mg. Pb and Hg peaks are easily identifiable following the sorption procedure.
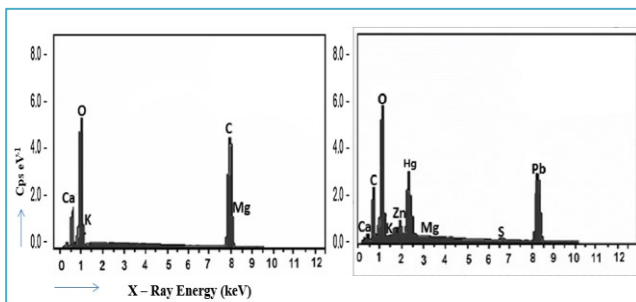
Figure 4. EDS spectra of water hyacinth before (a) and after (b) Pb and Hg adsorption
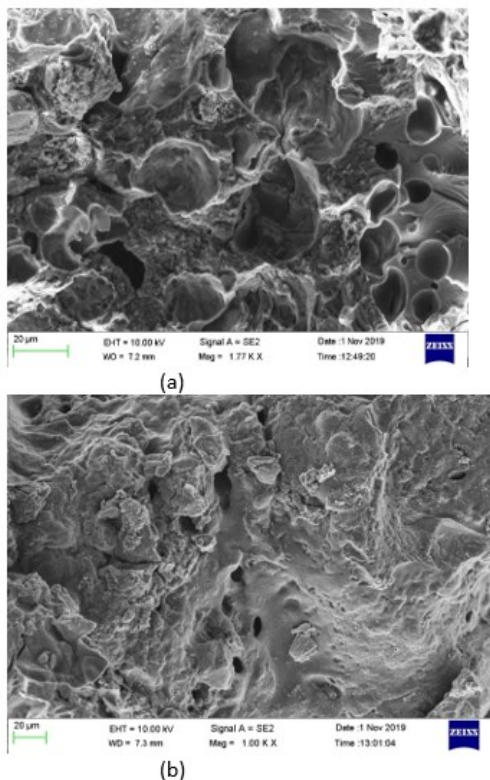

**Figure 5.** SEM morphology of water hyacinth before (a) and after (b) Pb and Hg adsorption

Figure 5 displays SEM typical images of the Water Hyacinth biochar both before and after the sorption of Pb and Hg. As the biosorbent interacts with lead (Pb) and mercury (Hg) during sorption, the outer layers undergo observable changes in their structure and appearance. Therefore, the clean biosorbents have fractured surfaces with uneven layers that could assist in the adsorption of Pb and Hg, in contrast to the more homogeneous water hyacinth biochar following sorption (Yogeshwaran *et al.* 2021).

3.2. Sorption tests

The adsorption of Pb and Hg ions (%R) was investigated at room temperature with an ideal pH of 4.5 and a contact time of 2 hours in batch study. In the Water hyacinth biochar approach the dose of 2 g/L with mass 0.05 g is applied, with the greatest removal percentage being around %R$_{max}$ = 92 and 99, respectively. %R$_{max}$ values are associated with the water hyacinth material's structure (Figure 6).
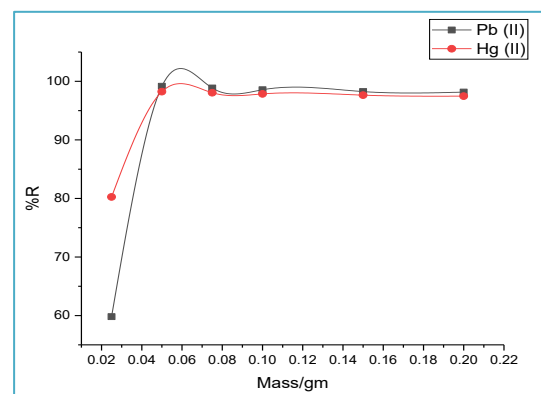
Figure 6. Pb and Hg removal (%R) as a function of hyacinth dose

This establishes the adsorbed species' distribution and site count. The isotherm studies were examined with metal ion concentration of C_0 = 27 – 197 mg/L, pH level of 4.5, and reaction time of 2 hours in room temperature. Figure 7 shows the experimental results for the Pb and Hg adsorption, q_e versus the equilibrium concentration C_e for Pb and Hg metal ions. Both the linear and nonlinear correlations in the data collected from experiments were fitted to the Freundlich and Langmuir models. The concave form of the isotherms that have been published (Figure 7) suggests that water hyacinth biochar is significantly effective for Pb and Hg sorption.
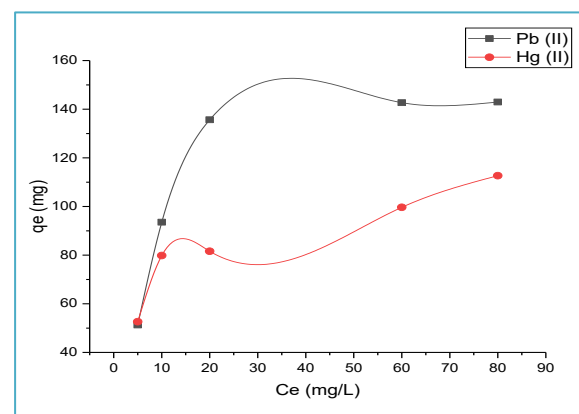
Figure 7. Isotherm non-linear fit of Pb and Hg adsorption using water hyacinth biosorbent

In the case of linear relationships, the experimental data of the isotherms were reformed as [log (q_e) vs. log (C_e)] and [C_e/q_e vs. C_e], which required adjustment using the Langmuir and Freundlich models, respectively. While the Freundlich model suggests multilayered adsorption with uneven sorption forces, the Langmuir model posits solute adsorption in single layers with a uniform sorption value (Fakhar *et al.* 2021). Isotherm adsorptions are better suited with the Langmuir model (R^2 = 0.97 & 0.96) than the Freundlich model (R^2 = 0.87 and 0.91), and they have higher R^2 values for linear correlations than for nonlinear correlations, according to Table 1, which also gives the parameters for both models' modifications (Saruchia *et al.* 2019). The initial model yields low K_L values, where the maximum sorption capacity (q_{max}) for Water Hyacinth biochar is equal to 158.7 and 123.5 mg Pb and Hg - biosorbent, respectively. These values show a strong affinity for Pb and Hg sorption. Even if the Freundlich model produced the worst adaptations, sorption procedures on uneven layers are still possible (Zhang *et al.* 2019). Pb and Hg are expended on water hyacinth biochar under favourable circumstances, determined by the proper 1/n adjustment ratios (between 0 and 1). All of these findings demonstrate that the sorption of Water Hyacinth biochar is a fairly complex process. It is noteworthy that Water Hyacinth biochar has some of the highest q_{max} values.

Table 1. Isotherm parameters for metal ion adsorption using Langmuir and Freundlich study

Isotherm study	Parameters	Measured Unit	Pb (II)	Hg (II)
Langmuir	q_{max}	mg/g	121.5	157.6
	K_L	1/mol	0.12	0.23
	R^2	-	0.972	0.960
Freundlich	K_f	L/g	43.84	24.67
	1/n	-	0.42	0.47
	R^2	-	0.871	0.912

3.3. Kinetic studies

The findings of the kinetic experiments carried out to determine the time of equilibrium required for Pb and Hg adsorption on water hyacinth biochar are shown in Figure 8. At time t (q_t), the amount of Pb and Hg eliminated per unit mass of biosorbent grows rapidly until it attains its highest level around 60 minutes afterwards. Almost constant qt is observed for longer times (t > 60). The adsorption kinetic data obtained from the experiment were calibrated using three different adsorption kinetic models: log (q_e - q_t) vs time t (a pseudo-first-order model); t/q_t vs. time t (a pseudo-second-order model); and q_t vs. $t^{1/2}$ (an intraparticle diffusion model). Table 2 reports the parameters that were acquired following the optimum changes along with the corresponding attributes (correlation coefficient effective R^2). Compared to the first-order adjustment models, we observe a stronger correlation (R^2 = 1) for both biosorbents with pseudo-second-order. As a result, we can confirm that: (i) Pb and Hg adsorption is a chemisorption process; (ii) computed adsorption capacities q_e, calculated agree well with experimentally observed adsorption capacities; and (iii)

adsorption rates (k_2 and h) for Water Hyacinth biochar (Adeogun *et al.* 2019).

(a)

(b)
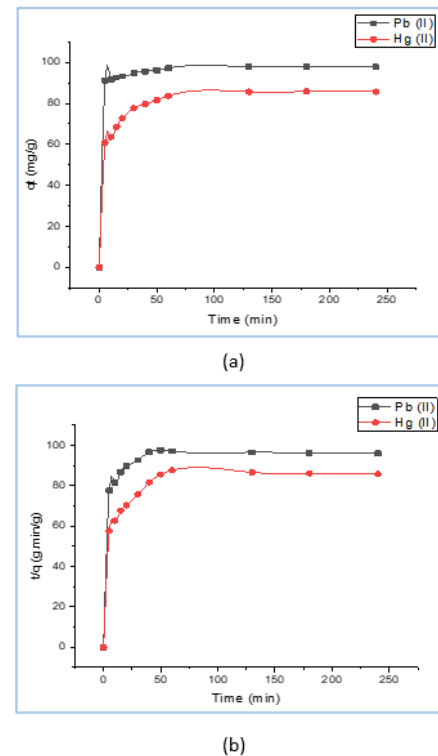
Figure 8. Adsorbed ions (q_t) versus time using Pseudo-first (a) and Pseudo-second order adjustments

The intra-particle diffusion model is fitted to the q_t vs. $t^{1/2}$ data for the Water Hyacinth biochar, as shown in Figure 9. Three components are discernible based on the kid intraparticle diffusion rate constants: In the first part, q_t grows quickly at time t (k_{id}, I > 3.7), suggesting that Pb and Hg ions are absorbed quickly on the biosorbents' exterior; in the second part, q_t grows more slowly at time t (0.16 < k_{id}, II < 3.3), suggesting that Pb and Hg ions enter and fill the biosorbent pores gradually (Obulapuram *et al.* 2021). The stage in enquiry is thought to govern the amount of dispersion to the mesopores (Marciniak *et al.* 2022). The third and final section, as indicated in Table 2, reveals that qt remains nearly constant with an extremely low kid, III values, suggesting that the rate-limiting step of the sorption process is intra-particle diffusion in micropores (Konicki *et al.* 2017). The desorption of Pb and Hg ions using various acids and regeneration cycles is shown in Figures 10 and 11.

Table 2. Experimental data calculated from kinetic studies for metal ion adsorption

Kinetic Model	Parameters	Pb (II)	Hg (II)
Pseudo – First order	k_1	0.03	0.08
	q_e (Cal)	19.54	7.68
	R^2	0.954	0.967
Pseudo – Second order	k_2	0.012	0.047
	q_e (Cal)	87.94	95.67
	h	47.5	319.5
	R^2	0.972	0.975
Intra – Particle Diffusion	K_{id} I	6.24	4.18
	K_{id} II	4.11	0.18
	K_{id} III	0.03	0.05
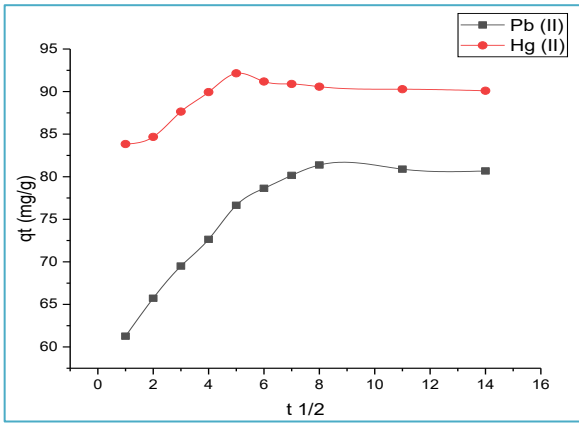
Figure 9. Pb and Hg adsorption using water hyacinth – Webber Morris plots
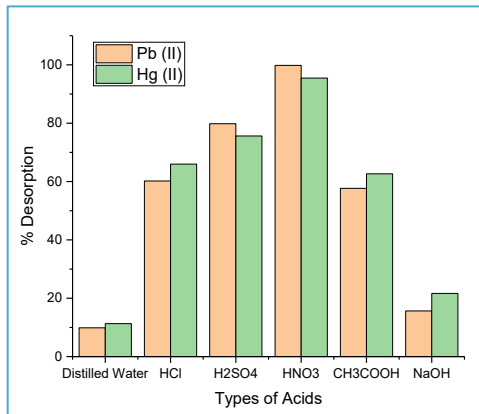

Figure 10. Desorption of Pb and Hg ions using various acids
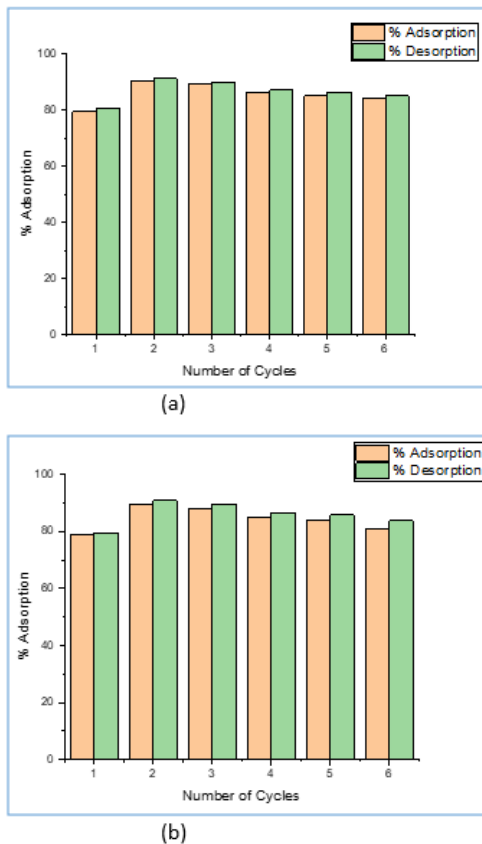
Figure 11. (a) & (b) Desorption and regeneration cycles for Pb and Hg metal ions

3.4. Adsorption thermodynamics

The synthetic solution was subjected to concentration variations of Pb(II) and Hg(II) ions between 20 and 60 mg/L. Thermodynamic analyses were carried out to evaluate the thermodynamic characteristics of the adsorption procedure. The thermodynamic charts of the chromium ion adsorption process at 10°C, 20°C, 30°C, and 40°C are shown in Figure 12. Table 3 displays the values of enthalpy (ΔH^o) and entropy (ΔS^o), which were obtained by taking the slope and intercept values out of the thermodynamic plots. The values of the Gibbs free energy (ΔG^o) at diverse temperatures are given in Table 3. Because the adsorption process utilizing water hyacinth biochar is spontaneous, the positive Gibbs energy values and negative enthalpy values confirm that the reaction is endothermic (Dulla *et al.* 2020). Furthermore, the absorption of Pb(II) and Hg(II) ions utilizing water hyacinth biochar material is unclear between the liquid and solid phases, as confirmed by the positive entropy values.
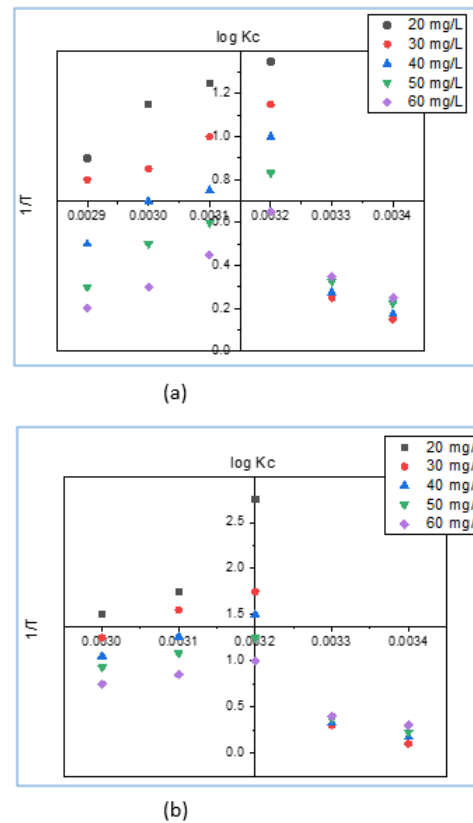
Figure 12. Thermodynamic plots for (a) Pb(II) and (b) Hg(II) metal ion adsorption using water hyacinth**CONCLUSION**

Agro-industrial waste biosorbents made of Water Hyacinth biochar were investigated for Pb and Hg sorption processes due to the desire to produce low-cost biomaterials for the removal of lead and mercury from contaminated waters. Zero charge point pH values (pH$_{zpc}$) for Water Hyacinth biochar e are 4.8 and 3.9, respectively. Before and after biosorption, IR spectra revealed variations in the strength and location of bands mostly connected to vibrational groups O-H, C-O, and C-O-C. Cracked surfaces with heterogeneous plates are visible in SEM/EDS analyses. Following Pb and Hg sorption, this morphology experiences notable alterations that lead to increased homogeneity.

For a mass of 0.05 g (dose=2 mg/L), at pH of 4.5, reaction time of 120 min, and ion concentration of 27 mg/L, water hyacinth biosorbent nearly achieve the maximum rate of metal ion removal (%R > 90). Based on the adsorption isotherms and modified Langmuir model, the maximum adsorption capacities (q_{max}) for Water Hyacinth biochar were determined to be 158.7 and 123.5 mg/g, respectively. The pseudo-second-order model precisely defines the sorption processes' kinetics. The related characteristics show that these are rapid processes of chemisorption,

especially for Water Hyacinth biochar (which is nearly six times greater than biosorbent). The most effective wastewater, according to desorption-regeneration tests, is HNO_3, from which Pb and Hg may be recovered up to more than 98% of the time (especially in the second cycle). The biosorbent water hyacinth biochar is reusable for a maximum of five times.

Table 3. Thermodynamic constants for Pb(II) and Hg(II) adsorption using water hyacinth

Type of metal ion	Concentration	ΔH°(KJ/mol)	ΔS°(J/mol)	ΔG$_o$ (kJ/mol)			
				15°C	30°C	45°C	60°C
Pb(II)	25	73.519	196.024	-13.106	-9.580	-8.362	-7.472
	30	41.822	101.345	-9.856	-8.532	-7.649	-6.328
	40	32.764	80.723	-8.299	-7.587	-7.116	-6.942
	50	20.134	42.542	-6.396	-6.244	-6.102	-5.632
	60	13.763	24.283	-5.457	-5.846	-5.125	-4.983
Hg(II)	25	45.434	113.234	-11.298	-9.438	-8.834	-6.683
	30	31.298	75.582	-9.462	-7.736	-7.336	-6.026
	40	26.442	56.983	-8.125	-6.906	-6.644	-5.519
	50	19.893	39.313	-7.622	-6.099	-5.383	-5.208
	60	13.298	28.921	-5.925	-5.028	-4.586	-4.224

References

A. K. Priya, V. Yogeshwaran, Saravanan Rajendran, Tuan K.A. Hoang, Matias Soto-Moscoso, Ayman A. Ghfar and Chinna Bathula (2022). Investigation of mechanism of heavy metals (Cr^{6+}, Pb_{2+}& Zn^{2+}) adsorption from aqueous medium using rice husk ash: Kinetic and thermodynamic approach, Chemosphere, 286, 131796. https://doi.org/10.1016/j.chemosphere.2021.131796

Abideen Idowu Adeogun (2019). Removal of methylene blue dye from aqueous solution using activated charcoal modified manganese ferrite (AC-MnFe$_2$O$_4$): kinetics, isotherms, and thermodynamics studies. Particulate Science and Technology, 38 (6), 756 – 767. https://doi.org/10.1080/02726351.2019.1626516

Ahmed Eleryan, Uyiosa O. Aigbe, Kingsley E. Ukhurebor, Robert B. Onyancha, Tarek M. Eldeeb, Mohamed A. El-Nemr, Mohamed A. Hassaan, Safaa Ragab, Otolorin A. Osibote, Heri S. Kusuma, Handoko Darmokoesoemo and Ahmed El Nemr (2022). Copper(II) ion removal by chemically and physically modified sawdust biochar. Biomass Conversion and Biorefinery. https://doi.org/10.1007/s13399-022-02918-y

Chuanbin Wang, Xutong Wang, Ning Li, Junyu Tao 2, Beibei Yan, Xiaoqiang Cui and Guanyi Chen (2022). Adsorption of Lead from Aqueous Solution by Biochar: A Review. Clean Technologies, 4, 629 – 652. https://doi.org/10.3390/cleantechnol4030039

Jie Hong, Junyu Xie, Seyyedali Mirshahghassemi, Jamie Lead (2020). Metal (Cu, Cr, Ni, Pb) removal from environmentally relevant waters using polyvinylpyrrolidone – coated magnetic nanoparticles. RSC advances, 10, 3266 – 3276. Doi: https://doi.org/10.1039/C9RA10104G

Jinzhen Ma, Liyuan Hou, Ping Li, Shumim Zhang and Xiangyu Zheng (2022). Modified fruit pericarp as an effective biosorbent for removing azo dye from aqueous solution: study of adsorption properties and mechanisms, Environmental Engineering Research, 27 (2), 200634. https://doi.org/10.4491/eer.2020.634

John Babu Dulla, Mohan Rao Tamana, Sumalatha Boddu, King Pulipati and Krupanidhi Srirama (2020). Biosorption of copper (II) onto spent biomass of Gelidiella acerosa (brown marine algae): optimization and kinetic studies, Applied Water Science, 10 (56). https://doi.org/10.1007/s13201-019-1125-3

Jyothi Kaparapu and M. Krishna Prasad (2018). Equilibrium, kinetics and thermodynamic studies of cadmium (II) biosorption on Nannochloropsis oculate, Applied Water Science, 8, 179. https://doi.org/10.1007/s13201-018-0810-y

Long Su, Haibo Zhang, Kokyo Oh, Na Liu, Yuan Luo, Hongyan Cheng, Guosheng Zhang and Xiaofang He (2021). Activated biochar derived from spent Auricularia auricula substrate for the efficient adsorption of cationic azo dyes from single and binary adsorptive systems, Water Science & Technology, 84 (1), 101 – 121. https://doi.org/10.2166/wst.2021.222

Manjuladevi M, Anitha R and Manonmani S (2018). Kinetic study on adsorption of Cr (VI), Ni (II), Cd (II) and Pb (II) ions from aqueous solutions using activated carbon prepared from cucumis melo peel. Applied water science, 8 (36) (2018). https://doi.org/10.1007/s13201-018-0674-1

Michal Marciniak, Joanna Goscianska, Małgorzata Norman, Teofil Jesionowski, Aleksandra Bazan-Wozniak and Robert Pietrzak (2022). Equilibrium, Kinetic, and Thermodynamic Studies on Adsorption of Rhodamine B from Aqueous Solutions Using Oxidized Mesoporous Carbons, Materials, 15, 5773. https://doi.org/10.3390/ma15165573

Mohammed Benjelloun, Youssef Miyah, Gulsun Akdemir Evrendilek, Farid Zerrouq Sanae Lairini (2021). Recent Advances in Adsorption Kinetic Models: Their Application to Dye Types, Arabian Journal of Chemistry, 14 (4), 103031. https://doi.org/10.1016/j.arabjc.2021.103031

Muhammad Mufazzal Saeed, Munir Ahmed (2020). Effect of temperature on kinetics and adsorption profile of endothermic chemisorption process: -tm (III) – PAN loaded

PUF system. Separation science and technology, 41, 705 – 722. Doi: https://doi.org/10.1080/01496390500527993

Narges samadani langeroodi, Zhaleh farhadravesh, Aliakbar dehno khalaji (2018) Optimization of adsorption parameters for Fe (III) ions removal from aqueous solutions by transition metal oxide nanocomposite. Green chemistry letters and reviews 11 (4): 404 – 413. Doi: https://doi.org/ 10.1080/17518253.2018.1526329

Nathalia Krummenauer Haro, Ivone Vanessa Jurado Dávila, Keila Guerra Pacheco Nunes, Marcela Andrea Espina de Franco, Nilson Romeu Marcilio and Liliana Amaral Féris (2021). Kinetic, equilibrium and thermodynamic studies of the adsorption of paracetamol in activated carbon in batch model and fixed-bed column, 11 (38). https://doi.org/10.1007/s13201-020-01346-5

Nida Fakhar, Suhail Ayoub Khan, Weqar Ahmad Siddiqi and Tabrez Alam Khan (2021). Ziziphus jujube waste-derived biomass as cost-effective adsorbent for the sequestration of Cd^{2+} from aqueous solution: Isotherm and kinetics studies. Environmental Nanotechnology, Monitoring & Management, 16, 100570. Doi: https://doi.org/10.1016/ j.enmm.2021.100570

Prasanna Kumar Obulapuram, Tanvir Arfin, Faruq Mohammad, Sachin K. Khiste, Murthy Chavali, Aisha N. Albalawi and Hamad A. Al-Lohedan (2021). Adsorption, Equilibrium Isotherm, and Thermodynamic Studies towards the Removal of Reactive Orange 16 Dye Using Cu(I)-Polyaninile Composite, Polymers, 13 (20), 3490. https://doi.org/10.3390/polym13203490

Saruchia and Vaneet Kumar (2019). Adsorption kinetics and isotherms for the removal of rhodamine B dye and Pb^{+2} ions from aqueous solutions by a hybrid ion-exchanger, Arabian Journal of Chemistry, 12 (3), 316 – 329. https://doi.org/10.1016/j.arabjc.2016.11.009

T. G. Ambaye, M. Vaccari, E. D. van Hullebusch, A. Amrane and S. Rtimi (2021). Mechanisms and adsorption capacities of biochar for the removal of organic and inorganic pollutants from industrial wastewater, International Journal of Environmental Science and Technology, 18, 3273 – 3294. https://doi.org/10.1007/s13762-020-03060-w

Tabrez Alam Khan, Md. Noumana, Divya Dua, Suhail Ayoub Khan, and Salman S. Alharthi (2022). Adsorptive scavenging of cationic dyes from aquatic phase by H_3PO_4 activated Indian jujube (Ziziphus mauritiana) seeds based activated carbon: Isotherm, kinetics, and thermodynamic study, Journal of Saudi Chemical Society, 26 (2), 101417. https://doi.org/10.1016/j.jscs.2021.101417

Wojciech Konicki, Małgorzata Aleksandrzak, Dariusz Moszyński and Ewa Mijowska (2017). Adsorption of anionic azo-dyes from aqueous solutions onto graphene oxide: Equilibrium, kinetic and thermodynamic studies, Journal of Colloid and Interface Science, 496, 188 – 200. https://doi.org/ 10.1016/j.jcis.2017.02.031

Xiaoran Zhang, Shimin Guo, Jungfeg Liu, Ziyang Zhang, Kaihong Song, Chaohong Tan, Haiyan Li (2019). A study on the removal of copper (II) from aqueous solution using lime sand bricks. Applied Sciences, 9 (4), 670. Doi: https://doi.org/10.3390/app9040670

Xutong Ma, Yiruo Liu, Qibo Zhang, Shaolong Sun, Xin Zhou and Yong Xu (2022). A novel natural lignocellulosic biosorbent of sunflower stem-pith for textile cationic dyes adsorption,

Journal of Cleaner Production, 331, 129878. https://doi.org/10.1016/j.jclepro.2021.129878

Y. Venkatraman and A.K. Priya (2021). Removal of heavy metal ion concentrations from the wastewater using tobacco leaves coated with iron oxide nanoparticles, International Journal of Environmental Science and Technology, 19, 2721–2736. https://doi.org/10.1007/s13762-021-03202-8

Yogeshwaran V and Priya A.K (2021). Experimental studies on the removal of heavy metal ion concentration using sugarcane bagasse in batch adsorption process. Desalination and Water Treatment, 224, 256 – 272. Doi: 10.5004/dwt.2021.27160